



Iranian Association of
Electrical and Electronics
Engineers

Journal of Applied Research in Electrical Engineering

E-ISSN: 2783-2864

P-ISSN: 2717-414X

Homepage: <https://jaree.scu.ac.ir/>



Research Article

Comparative Analysis of Lithium-ion Battery for Long and Short Pulse Discharge Experiments in State-of-Charge Estimation with Extended Kalman Filter

Behnam Ersi Alambaz¹ , Mohsen Ghalehnoie^{1,*} , and Hamid Reza Moazami²

¹ Faculty of Electrical Engineering Shahrood University of Technology, Shahrood, Iran.

² Nuclear Fuel Cycle Research School, Energy Science and Technology Research Institute, Tehran, Iran.

* Corresponding Author: ghalehnoie@shahroodut.ac.ir

Abstract: This paper explores the impact of two types of experiments, known as "long pulse" and "short pulse," experiments, on identifying models for Lithium-ion batteries. The focus is on improving the estimation of the state of charge (SoC) using an extended Kalman filter. The results consistently demonstrate that applying the extended Kalman filter to models identified through long pulse experiments outperforms those identified through short pulse experiments in estimating battery SoC and terminal voltage. The article delves into the reasons for this improvement from both circuit and electrochemical perspectives, providing insights into the obtained results. Thus, the study advocates for the preference of long pulse strategies to enhance the performance of Lithium-ion batteries, offering insights that contribute to the development of innovative and sustainable energy storage solutions.

Keywords: Lithium-ion batteries, long-pulse, short-pulse, state of charge

Article history

Received xxx; Revised xxx; Accepted xxx; Published online 30 October.

© 20xx Published by Shahid Chamran University of Ahvaz & Iranian Association of Electrical and Electronics Engineers (IAEEE)

How to cite this article

B. Ersi Alambaz, M. Ghalehnoie, and H. R. Moazami, "Comparative Analysis of Lithium-ion Battery for Long and Short Pulse Discharge Experiments in State-of-Charge Estimation with Extended Kalman Filter," *J. Appl. Res. Electr. Eng.*, Vol. 3, No. 2, pp. 201-207, 2024. DOI: 10.22055/jaree.2024.46715.1117



1. INTRODUCTION

Lithium-ion batteries (LIBs) have become indispensable components not only in portable electronics and electric vehicles but also in advanced energy systems like microgrids, where they contribute to frequency control and energy management through fast-response capabilities [1]. The integration of LIBs in such systems underscores their versatility and critical role in ensuring stability and efficiency, especially in scenarios where precise energy balance is paramount. The precise estimation of the state of charge (SoC) in LIBs plays a pivotal role in battery management systems, directly influencing their overall performance and lifespan. As Lithium-ion batteries find extensive applications in electric vehicles and portable electronics, ensuring reliable and accurate SoC estimation becomes imperative for optimizing their usage and achieving efficient energy management. A plethora of techniques have been devised to tackle the SoC estimation challenge,

encompassing methods such as coulomb counting [2], neural networks [3], and model-based observers [4]. Notably, among the model-based observers, the extended Kalman filter (EKF) has gained substantial attention from researchers due to its adeptness in assimilating system dynamics and uncertainties. However, the performance of traditional EKF-based approaches can degrade under dynamic operating conditions, leading to the development of more robust methods, such as the modified adaptive extended Kalman filter (MAEKF), which incorporates adaptive mechanisms to address transient disturbances and bias issues [5]. This adaptability empowers the EKF to deliver more precise and robust SoC predictions.

Model-based observers demand a dynamic model that aptly represents the intricate behavior of the battery. This dynamic model can take various forms, such as an electrochemical model [6], a neural network model [7], or an equivalent circuit model [8]. Electrochemical models, renowned for their detailed representation of battery physics, often require substantial computational resources, limiting

their real-time applicability. Neural network models, while exhibiting promise in certain applications, face challenges in providing transparent insights into the underlying battery behavior. The "black-box" nature of neural networks makes it challenging to interpret the model's decisions, hindering their utility in safety-critical applications where understanding the reasoning behind predictions is paramount. Moreover, neural networks may struggle with generalization across a wide range of operating conditions, limiting their effectiveness in dynamic and diverse battery environments.

In contrast, equivalent circuit models [9] have gained widespread acceptance due to their ability to strike a harmonious balance between accuracy and computational efficiency. Their simplified yet effective representation of electrochemical processes makes them suitable for real-time applications, providing precise SoC estimates without compromising speed. This popularity underscores the pragmatic advantages of equivalent circuit models in delivering reliable and efficient solutions for Lithium-ion battery management systems.

Despite these advantages, one potential drawback of equivalent circuit models is their reliance on accurate parameter identification, which can be sensitive to variations in operating conditions. Additionally, while integer-order models are simpler and computationally efficient, they may lack the flexibility to capture more complex battery dynamics, which could be addressed in future work by exploring fractional-order models or incorporating advanced machine learning techniques.

Equivalent circuit models play a pivotal role in estimating SoC in LIBs, offering flexibility to represent various configurations, from single-cell [10] to multi-cell [11] setups. The selection of model complexity, whether single-cell or multi-cell, involves a trade-off between computational efficiency and accuracy. Single-cell models, while computationally efficient, may oversimplify the intricate behavior of LIBs, leading to inaccuracies in predicting responses during dynamic conditions. The simplicity of these models comes at the cost of potentially overlooking crucial nuances in the battery's behavior. On the other hand, multi-cell models capture system-level dynamics but encounter challenges when applied to individual cells, especially in the presence of pulse-related phenomena. The complexities introduced by inter-cell interactions and the difficulty in accurately extrapolating system-level behaviors to individual cells can compromise the accuracy of predictions. To address these challenges, advanced techniques such as the three-time-scale dual extended Kalman filtering method have been developed, which enables more accurate parameter and state estimation by adjusting the sampling time based on the impact of each parameter on terminal voltage [12]. This method enhances the model's ability to accurately represent the dynamic behavior of LIBs, particularly under varying operational conditions.

However, the dynamics of these equivalent circuit models can be expressed in terms of integer-order or fractional-order derivatives. While fractional-order models offer increased complexity, their adoption faces challenges in parameter identification and computational efficiency. The fractionalization introduces intricacies, making the identification of model parameters more complex. In light of

these considerations, the prevailing preference leans towards integer-order dual-cell models. These models involve parameters that require identification based on battery voltage and current under various experimental conditions. Common methods for parameter identification include short pulse and long pulse experiments, each offering insights into the dual-cell model's behavior under specific dynamic conditions.

This research aims to refine the state of charge (SoC) estimation in Lithium-ion batteries by employing an integer-order dynamic model. By conducting separate pulse experiments—long pulses and short pulses—we identify parameters for the dynamic model. This approach yields two distinct models, one from each experiment, offering flexibility in Kalman filter application for SoC estimation. The results reveal that models derived from long pulse experiments generally exhibit higher accuracy, providing crucial guidance for model selection under various battery operating conditions. This nuanced approach enhances the precision of SoC estimation, contributing valuable insights to Lithium-ion battery management systems.

The paper unfolds in a structured manner, commencing with the extraction of an integer-order dynamic model for a dual-cell equivalent circuit in the section 2. Section 3 delves into the intricacies of parameter identification, encompassing the identification of open-circuit voltage, internal resistance, and other battery parameters. Following this, the results obtained from data acquired in both long pulse and short pulse experiments for parameter estimation are presented. The estimation outcomes, achieved by deploying an extended Kalman filter on each model, are thoroughly compared. The concluding section encapsulates the key findings and insights derived from the study.

2. DYNAMIC MODELING OF LITHIUM-ION BATTERIES

We highlighted the significance of equivalent electrical circuit models for lithium-ion batteries and addressed the limitations of both single-cell and multi-cell models. Recognizing these challenges, the focus shifted towards a prevalent solution—the dual-cell electrical equivalent circuit, renowned for its effectiveness in capturing the battery's dynamic behavior (refer to Fig. 1). This model incorporates crucial elements, such as internal resistance (R_0), polarization resistances due to electrochemical polarization (R_1 and R_2), and polarization capacitances (C_1 and C_2).

The dual-cell model is expressed through a set of dynamic equations that govern the system's continuous-time behavior. Let's consider the following components and variables:

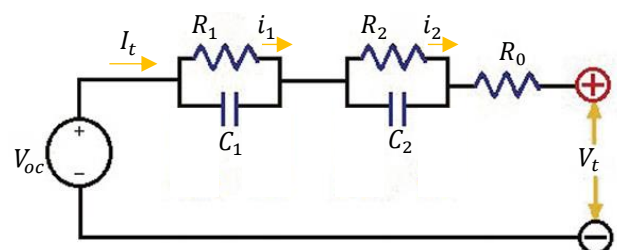


Fig. 1. Two-cell equivalent circuit model for LIBs.

i_1, i_2 : Currents through R_1 and R_2 , respectively.
 SOC : State of charge, the battery's charge level.
 V_t : Terminal voltage.
 I_t : Terminal current.
 V_{OC} : Open-circuit voltage, depends on the SOC .

$$SOC(t) = SOC(0) - \frac{1}{C_n} \int_0^t I_t(t) dt, \quad (1)$$

where C_n is the nominal capacity of battery. Using Kirchhoff's laws, Ohm's law, and the definition of state of charge (1), the continuous-time dynamic equations for the dual-cell model are given by:

$$\frac{di_1}{dt} = -\frac{1}{R_1 C_1} i_1 + \frac{1}{R_1 C_1} I_t, \quad (2)$$

$$\frac{di_2}{dt} = -\frac{1}{R_2 C_2} i_2 + \frac{1}{R_2 C_2} I_t, \quad (3)$$

$$\frac{dSOC}{dt} = -\frac{I_t(t)}{C_n}, \quad (4)$$

and the output equation is,

$$V_t(t) = -R_1 i_1 - R_2 i_2 - R_0 I_t + V_{OC}(SOC) \quad (5)$$

The dynamic equations (2)-(4) governing the derivatives of the state variables in the battery system are linear. However, the output equation becomes non-linear due to the dependence of the open-circuit voltage (V_{OC}) on the state of charge (SOC), and as a result, the entire battery system can be considered non-linear when viewed from the input current (I_t) to the output voltage (V_t). Consequently, in the subsequent sections, an extended Kalman filter technique is employed to estimate the state of charge. To facilitate the application of the extended Kalman filter, these continuous-time equations (2)-(5) are discretized using the Euler method with a sampling rate Δt , resulting in the following discrete-time system equations:

$$\begin{bmatrix} i_1(k+1) \\ i_2(k+1) \\ SOC(k+1) \end{bmatrix} = A \begin{bmatrix} i_1(k) \\ i_2(k) \\ SOC(k) \end{bmatrix} + \begin{bmatrix} 1 - \exp\left(\frac{-\Delta t}{R_1 C_1}\right) \\ 1 - \exp\left(\frac{-\Delta t}{R_2 C_2}\right) \\ \frac{-\Delta t}{C_n} \end{bmatrix} I_t(k), \quad (6)$$

$$V_t(k+1) = C \begin{bmatrix} i_1(k) \\ i_2(k) \\ SOC(k) \end{bmatrix} - R_0 I_t(k) + V_{OC}(SOC(k)), \quad (7)$$

where,

$$A = \begin{bmatrix} \exp\left(\frac{-\Delta t}{R_1 C_1}\right) & 0 & 0 \\ 0 & \exp\left(\frac{-\Delta t}{R_2 C_2}\right) & 0 \\ 0 & 0 & 1 \end{bmatrix}, \quad (8)$$

$$C = [-R_1 \quad -R_2 \quad 0] \quad (9)$$

3. PARAMETER ESTIMATION

In the previous section, we developed the dynamic equations of a lithium-ion battery based on a dual-cell equivalent circuit model, which includes parameters that require identification for accurate representation. Two

methods, the long pulse and short pulse experiments, are employed for parameter identification. Here, we provide further insights into these experiments and present the terminal current and voltage profiles for both scenarios in Fig. 2 and Fig. 3 (both refer to short and long terminal current, respectively), although Fig. 4 and Fig. 5 (both refer to long and short terminal voltage, respectively), for a commercially available Maxell ER3 14250 lithium-ion battery (Japan) with a nominal capacity of 500mAh and nominal voltage of 3.7 volts. The battery under examination has a maximum voltage of 4.2 volts and a cut-off voltage of 3 volts. The testing procedure involve cycling the battery at a temperature of 25°C.

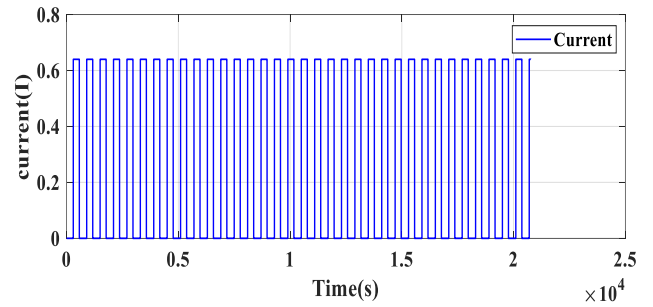


Fig. 2. Terminal current during Short Pulse experiments.

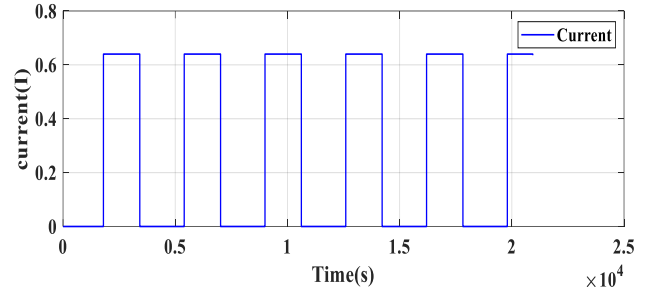


Fig. 3. Terminal current during Long Pulse experiments.

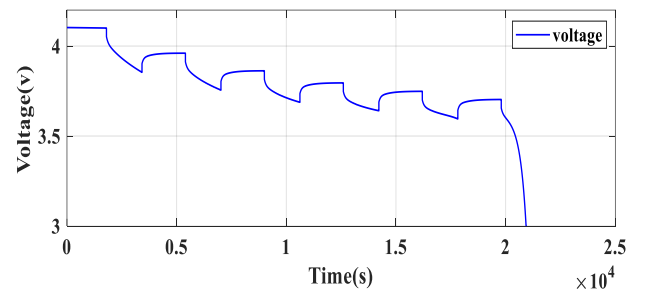


Fig. 4. Terminal voltage during Long Pulse experiments.

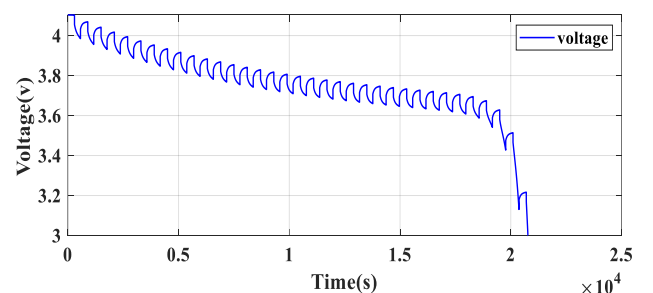


Fig. 5. Terminal voltage during Short Pulse experiments.

Utilizing these precise current measurements, the state of charge (SOC) at each time step, especially at the end of the resting period, is determined using Equation (1).

For instance, considering the magnitude of the current drawn from the battery and its duration in the long pulse experiment, it can be observed that during each discharge and rest cycle, 10% of the battery charge is depleted. Consequently, since the battery starts with a full charge, the battery charge level decreases to 0.9 at the end of the rest cycle after the first discharge and continues to decrease to 0.8 at the end of the subsequent cycle, and so forth. So, considering that no current flows during resting intervals, and the battery is in a quiescent state, according to applying the voltage Kirchhoff's law, it is expected that the voltages across the RC branches become zero, resulting in the terminal voltage being equal to the open-circuit voltage (V_{OC}).

When V_{OC} as a function of SOC identified, the next step is to estimate the internal resistance (R_0) (according to the figure 6) using the following method during discharge-rest intervals [13]:

$$R_0 = \frac{(V_A - V_B) + (V_D - V_C)}{2I_t} \quad (10)$$

in which V_A , V_B , V_C , and V_D represent the battery voltages during each time interval corresponding to discharge and rest, as illustrated in Fig. 6. For further details, please refer to [14]. In this way, the identified value for R_0 in this study are 0.0749 ohms and 0.0748 ohms for long pulse and short pulse experiments, respectively. This indicates that the type of experiment does not have a significant impact on estimating the internal resistance of the battery.

Now, armed with V_{OC} and R_0 , the relationship between the terminal currents and the output voltage (y , voltage of the total cells) for the dual-cell model can be established. By leveraging the ARX [15] or ARMAX [16] techniques, the transfer function from the output y to the input I_t is obtained.

$$\frac{Y}{I_t} = \frac{b_1q^{-1} + b_2q^{-2}}{1 + a_1q^{-1} + a_2q^{-2}} \quad (11)$$

Comparing this identified system with the ARX model, considering the system's governing equations akin to Equations (2)-(5), and considering the output as the voltage across the cell terminals (y):

$$y = [-R_1 \quad -R_2 \quad 0] \begin{bmatrix} \dot{i}_{1,k} \\ \dot{i}_{2,k} \\ SOC_k \end{bmatrix} + (-R_0)I_k, \quad (12)$$

the parameterized system transfer function becomes:

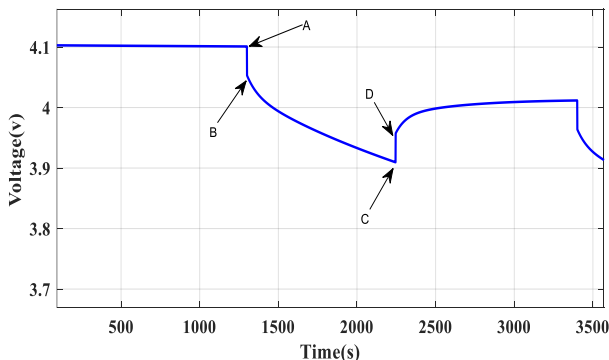


Fig. 6. Voltage profile during a discharge-rest cycle in both long and short pulse experiments.

$$\frac{Y}{I_t} = \frac{A(q^{-1})}{B(q^{-1})}, \quad (13)$$

$$A(q^{-1}) = (R_1 + R_2 - R_1\sigma_2 - R_2\sigma_1)q^{-2} + (R_1\sigma_2\sigma_1 - R_1\sigma_1 - R_2\sigma_2 + R_2\sigma_2\sigma_1)q^{-1} \quad (14)$$

$$B(q^{-1}) = q^{-2} + (-\sigma_2 - \sigma_1)q^{-1} + \sigma_2\sigma_1 \quad (15)$$

$$\sigma_1 = \exp\left(\frac{-\Delta t}{R_1C_1}\right) \quad (16)$$

$$\sigma_2 = \exp\left(\frac{-\Delta t}{R_2C_2}\right) \quad (17)$$

Comparison between the identified system and the ARX system yields,

$$R_1 = -\frac{2}{a_1 + \sqrt{a_1^2 - 4}}, \quad (18)$$

$$R_2 = \frac{a_1 + \sqrt{a_1^2 - 4}}{-2}, \quad (19)$$

$$\sigma_1 = \frac{1}{e^{C_2R_2}}, \quad (20)$$

$$\sigma_2 = \frac{1}{e^{C_1R_1}}, \quad (21)$$

$$C_1 = \frac{1}{\sigma_1 \cdot R_1}, \quad (22)$$

$$C_2 = \frac{1}{\sigma_2 \cdot R_2}, \quad (23)$$

This comprehensive approach ensures the accurate identification of key parameters and validates the dual-cell model's efficacy. The obtained parameters based on this method are summarized in Table 1.

4. STATE OF CHARGE ESTIMATION

The extended Kalman filter (EKF) [17], [18] is known as a widely used technique to estimate the state of charge (SoC) and state of health (SoH) in Li-ion) battery systems. EKF, which acts as a recursive algorithm, uses a mathematical model to predict battery behavior and compares it with measured data, facilitating the estimation of internal parameters in the battery model. As an extension of the Kalman filter, the EKF is a special value system with nonlinear dynamics. The EKF algorithm consists of two main steps: the prediction step and the update step. During the prediction phase, the battery model predicts the behavior of the system in a short period based on the current state of the battery, with known inputs such as current and voltage as outputs for this estimation phase. This output includes the battery status and its covariance. Afterwards, in the update step, the measured data from the battery system is used to adjust the predicted state estimate. The Kalman gain, which acts as a weighting factor, determines the influence of the

Table 1: Summary of identified battery parameters using different experimental methods.

Experiment	Long Pulse	Short Pulse
R_1 (ohm)	0.0496	0.0455
R_2 (ohm)	0.0473	0.0509
C_1 (farad)	664.64	707.73
C_2 (farad)	4.83×10^3	4.30×10^3

predicted state estimate and the measured data in determining the updated state estimate.

This updated state estimate then serves as the initial state for the next prediction step. EKF has proven to be useful in estimating SoC and SoH [19] in Li-ion battery systems, primarily due to its ability to accommodate nonlinearities in the battery model. This includes factors such as changes in battery capacity as a function of temperature [20] and state of charge. The choice of the battery model, which can be physics-based or empirical, depends on the desired level of accuracy. (Fig. 7 to Fig. 12) provide a quantitative representation of the EKF program under different pulsing

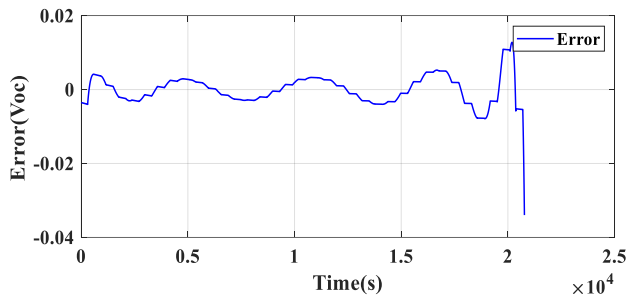


Fig. 7. Open circuit voltage error in short pulse mode.

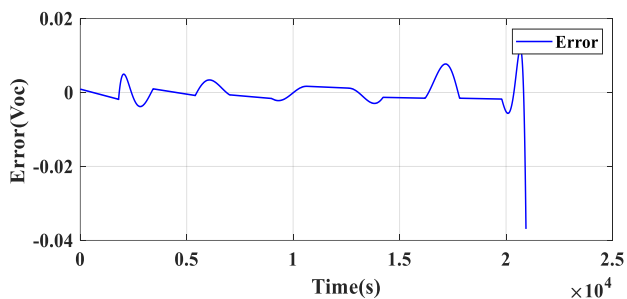


Fig. 8. Open circuit voltage error in long pulse mode.

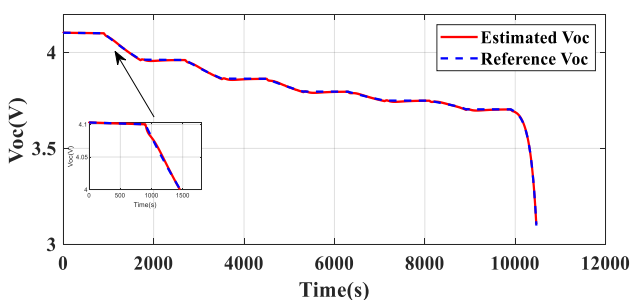


Fig. 9. Actual (solid line) and estimated (dashed line) values of open circuit voltage in long pulse mode.

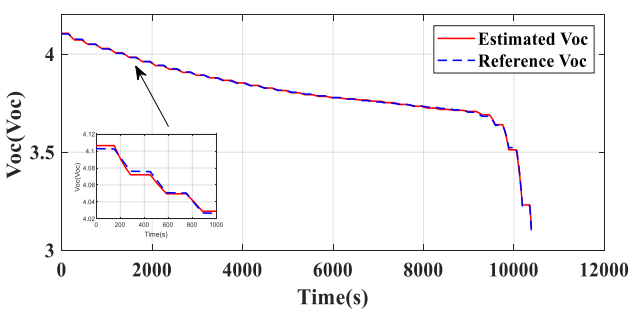


Fig. 10. Actual (solid line) and estimated (dashed line) values of open circuit voltage in short pulse mode.

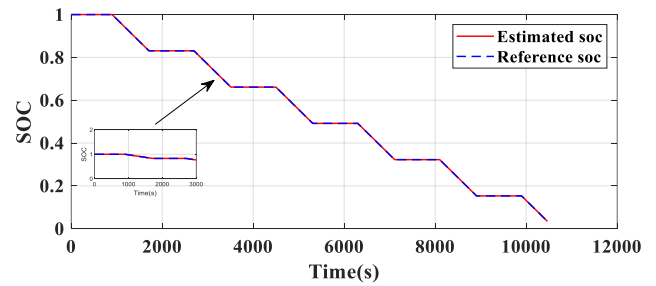


Fig. 11. Actual (solid line) and estimated (dashed line) values of SOC in long pulse mode.

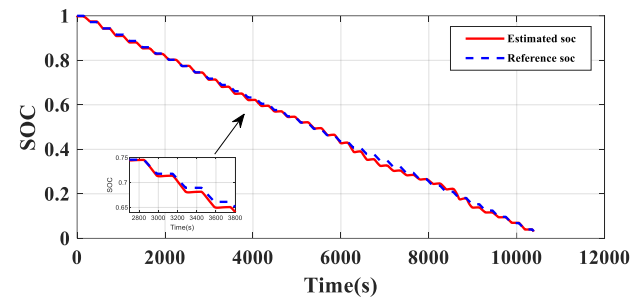


Fig. 12. Actual (solid line) and estimated (dashed line) values of SOC in short pulse mode.

conditions and optimization. It helps with battery performance and battery life. The robustness of EKF makes it a potential tool for real-time battery management applications in electric vehicles and renewable energy systems.

As seen in Fig. 7 and Fig. 8, the open circuit voltage error is evident in both short pulse and long pulse conditions. At the beginning of the current cycle, the extracted error value is lower in the short pulse condition. It can be concluded that the stability of the Li-ion battery is compromised by short cycles, starting at 100% charge, but as the current cycle continues and the central core of the Li-ion battery heats up, as shown in Fig. 10 and Fig. 12, the modeling errors appear during the short pulse cycle of the open circuit voltage and state of charge of the Li-ion battery.

Conversely, long pulses exhibit stable performance within the performance range of Li-ion batteries due to their longer rest intervals that allow the core to cool down in each current cycle and prepare the battery memory for the next cycle. This range extends from 70% to 30% under voltage 3.8 to 3.3, as clearly seen in Fig. 9 and Fig. 11. The observer estimated battery performance much more accurately in open circuit voltage and battery state of charge compared to short pulse conditions.

5. CONCLUSION

In conclusion, the exploration of open-circuit voltage errors under short and long-pulse conditions, as detailed in this conference paper, reveals a captivating narrative. Initially, there is an observation of lower error magnitudes in short-pulse scenarios. However, a nuanced trend emerges, highlighting that the system's accuracy diminishes with an increasing number of current flow and discharge cycles, especially in short-pulse conditions. Introducing the consideration of the charging state adds complexity to the

analysis. In long-pulse scenarios, due to the longer rest time, there is a nearly 5RC duration where a higher confidence in the equality of terminal voltage and open-circuit voltage is observed at the end of each rest cycle. Despite these advancements, one limitation of the current study is the potential for parameter drift over extended operation cycles, which could impact the long-term accuracy of the SoC estimation. Future work should explore adaptive estimation techniques or machine learning approaches that can dynamically adjust model parameters to account for such variations. Furthermore, the discussion extends to the topic of open-circuit voltage errors and the level of precision in estimating the state of charge in both short-pulse and long-pulse scenarios. It is noteworthy that in short-pulse conditions, the next significant aspect to be addressed is the accuracy of voltage circuit errors and the precision of the estimator in assessing the battery's charge state. These detailed insights contribute to a more comprehensive understanding of system dynamics, offering valuable considerations for the optimization of open circuit voltage configurations and charging state estimation in battery

REFERENCES

- [1] S. Aminzadeh, M. T. Hagh, and H. Seyedi, "Journal of Applied Research in Electrical Engineering Reactive Power Coordination Between Solid Oxide Fuel Cell and Battery for Microgrid Frequency Control," vol. 1, no. 2, pp. 121–130, 2022.
- [2] K. Propp, D. J. Auger, A. Fotouhi, S. Longo, and V. Knap, "Kalman-variant estimators for state of charge in lithium-sulfur batteries," *J. Power Sources*, vol. 343, pp. 254–267, 2017.
- [3] M. Jiao, D. Wang, and J. Qiu, "A GRU-RNN based momentum optimized algorithm for SOC estimation," *J. Power Sources*, vol. 459, 2020.
- [4] D. Nissing and H. S. Birnale, "Core temperature observer design and model parameter uncertainty analysis for a lithium battery," *IFAC-PapersOnLine*, vol. 53, no. 2, pp. 12505–12510, 2020.
- [5] S. Rout and S. Das, "A robust modified adaptive extended Kalman filter for state-of-charge estimation of rechargeable battery under dynamic operating condition," *Electr. Eng.*, 2024.
- [6] K. S. R. Mawonou, A. Eddahech, D. Dumur, D. Beauvois, and E. Godoy, "Improved state of charge estimation for Li-ion batteries using fractional order extended Kalman filter," *J. Power Sources*, vol. 435, no. March, p. 226710, 2019.
- [7] A. Pooladvand and D. A. Abolmasoumi, "Dynamic State Estimation of Micro-grids by Using Accelerated Particle Filters," p. 99, 2020.
- [8] Z. Ren and C. Du, "State of Charge Estimation for Lithium-ion Batteries using Extreme Learning Machine and Extended Kalman Filter," *IFAC-PapersOnLine*, vol. 55, no. 24, pp. 197–202, 2022.
- [9] X. Jiang, B. Zhang, Y. Wang, Y. Xiang, and W. Li, systems. As we advance, this research sets the stage for further studies and advancements in the field, enriching the knowledge base for future developments.

CREDIT AUTHORSHIP CONTRIBUTION STATEMENT

Behnam Ersi Alambaz: Conceptualization, Formal analysis, Methodology, Software, Roles/Writing - original draft, Writing - review & editing. **Mohsen Ghalehnoie:** Conceptualization, , Formal analysis, Methodology , Supervision, Validation, Roles/Writing - original draft, Writing - review & editing. **Hamid Reza Moazami:** Formal analysis, Methodology, Supervision, Validation, Writing - review & editing.

DECLARATION OF COMPETING INTEREST

The authors declare that they have no known competing financial interests or personal relationships that could have appeared to influence the work reported in this paper. The ethical issues; including plagiarism, informed consent, misconduct, data fabrication and/or falsification, double publication and/or submission, redundancy has been completely observed by the authors.

"Modeling and state of charge estimation of Lithium-ion Battery using the autoregressive exogenous model," *2020 IEEE 1st China Int. Youth Conf. Electr. Eng. CIYCEE 2020*, pp. 1–7, 2020.

- [10] X. Li and S. Y. Choe, "State-of-charge (SOC) estimation based on a reduced order electrochemical thermal model and extended Kalman filter," *Proc. Am. Control Conf.*, pp. 1100–1105, 2013.
- [11] X. Hu, S. Li, and H. Peng, "A comparative study of equivalent circuit models for Li-ion batteries," *J. Power Sources*, vol. 198, pp. 359–367, 2012.
- [12] M. Zhu, K. Qian, and X. Liu, "A three-time-scale dual extended Kalman filtering for parameter and state estimation of Li-ion battery," *Proc. Inst. Mech. Eng. Part D J. Automob. Eng.*, vol. 238, no. 6, pp. 1352–1367, 2024.
- [13] J. Lv, B. Jiang, X. Wang, Y. Liu, and Y. Fu, "Estimation of the state of charge of lithium batteries based on adaptive unscented Kalman filter algorithm," *Electron.*, vol. 9, no. 9, pp. 1–22, 2020.
- [14] L. Rozaqi and E. Rijanto, "SOC estimation for Li-ion battery using optimum RLS method based on genetic algorithm," *Proc. 2016 8th Int. Conf. Inf. Technol. Electr. Eng. Empower. Technol. Better Futur. ICITEE 2016*, 2017.
- [15] X. K. Chen and D. Sun, "Modeling and state of charge estimation of lithium-ion battery," *Adv. Manuf.*, vol. 3, no. 3, pp. 202–211, 2015.
- [16] A. Kaleli and H. İ. Akolaş, "Recursive ARMAX-Based Global Battery SOC Estimation Model Design using Kalman Filter with Optimized Parameters by Radial Movement Optimization Method," *Electr. Power Components Syst.*, vol. 51, no. 11, pp. 1027–1039, Jul. 2023.
- [17] W. Bai, X. Zhang, Z. Gao, S. Xie, K. Peng, and Y. Chen, "Sensorless Coestimation of Temperature and State-of-

Charge for Lithium-Ion Batteries Based on a Coupled Electrothermal Model,” *Int. J. Energy Res.*, vol. 2023, pp. 1–18, 2023.

- [18] T. Sun, R. Wu, Y. Cui, and Y. Zheng, “Sequent extended Kalman filter capacity estimation method for lithium-ion batteries based on discrete battery aging model and support vector machine,” *J. Energy Storage*, vol. 39, no. May, p. 102594, 2021.
- [19] X. Wei, M. Yimin, and Z. Feng, “Identification of Parameters in Li-Ion Battery Model by Least Squares Method with Variable Forgetting Factor,” *Int. J. Comput. Methods*, vol. 17, no. 7, pp. 1–20, 2020.
- [20] J. Sun *et al.*, “Online internal temperature estimation for lithium-ion batteries based on Kalman filter,” *Energies*, vol. 8, no. 5, pp. 4400–4415, 2015.

BIOGRAPHY



Behnam Ersi Alambaz was born in Mazandaran, Iran in 1994. He finished his M.Sc. in electrical control engineering at Shahrood University of Technology, Shahrood, Iran. His research interested are control and system identification.



Mohsen Ghalehnoie was born in Shahrood, Iran, in 1982, and holds Bachelor's, Master's, and Doctoral degrees in control engineering. He earned his B.Sc. and M.Sc. degrees from Iran University of Science and the University of Tehran in 2005 and 2008, respectively. Additionally, he received his Ph.D. from Ferdowsi University of Mashhad in 2018. Currently, he serves as an assistant professor of control engineering at Shahrood University of Technology, Shahrood, Iran. His work focuses on control systems theory, optimization, fuzzy control, data fusion, and expert systems, especially for hybrid switched systems and industrial processes.



Hamid Reza Moazami received his bachelor's degree in Applied Chemistry from Isfahan University of Technology in 2002, and his master's degree in Analytical Chemistry from Tehran University in 2005. He received his PhD in Analytical Chemistry from the Shahid University in 2015. He is currently an assistant Professor at Nuclear Science and Technology Research Institute. His research focuses on the development of novel electrochemical systems for energy and environmental applications.

Copyrights

© 20xx by the author(s). Licensee Shahid Chamran University of Ahvaz, Ahvaz, Iran. This article is an open-access article distributed under the terms and conditions of the Creative Commons Attribution –NonCommercial 4.0 International (CC BY-NC 4.0) License (<http://creativecommons.org/licenses/by-nc/4.0/>).

